JCTC Journal of Chemical Theory and Computation

A Scheme for the Evaluation of Electron Delocalization and Conjugation Efficiency in Linearly π-Conjugated Systems

Maurizio Bruschi,[†] Peter A. Limacher,[‡] Jürg Hutter,[§] and Hans Peter Lüthi[‡,*]

Department of Environmental Science, Università degli Studi di Milano-Bicocca, Piazza della Scienza 1, I-20126 Milano, Italy; Laboratory for Physical Chemistry, ETH Zürich, Wolfgang-Pauli-Strasse 10, CH-8093 Zürich, Switzerland; and Physical Chemisty Institute, University of Zürich, Winterthurerstrasse 190, CH-8057 Zürich, Switzerland

Abstract: In this study, we present a scheme for the evaluation of electron delocalization and conjugation efficiency in lineraly π-conjugated systems. The scheme, based on the natural bond orbital theory, allows monitoring the evolution of electron delocalization along an extended conjugation path as well as its response to chemical modification. The scheme presented is evaluated and illustrated by means of a computational investigation of π-conjugation in *all-trans* polyacetylene [PA; $H(-CH=CH)_n-H$], polydiacetylene [PDA, $H(-C\equiv C-CH=CH)_n-H$], and polytriacetylene [PTA, $H(-C\equiv C-CH=CH-C\equiv C)_n-H$] with up to 180 carbon atoms, all related by the number of ethynyl units incorporated in the chain. We are able to show that for short oligomers the incorporation of ethynyl spacers into the PA chain increases the π-delocalization energy, but, on the other hand, reduces the efficiency with which π-electron delocalization is promoted along the backbone. This explains the generally shorter effective conjugation lengths observed for the properties of the polyeneynes (PDA and PTA) relative to the polyenes (PA). It will also be shown that the reduced conjugation efficiency, within the NBO-based model presented in this work, can be related to the orbital interaction pattern along the π-conjugated chain. We will show that the orbital interaction energy pattern is characteristic for the type and the length of the backbone and may therefore serve as a descriptor for linearly π-conjugated chains.

1. Introduction

For the rational design of functionalized π-conjugated polymers, which are extensively being investigated as materials for application in nanoscience, molecular electronics, photonics, and other areas,[1,2] a more thorough understanding of electron delocalization and conjugation efficiency is crucial. In this class of materials, polyacetylene [PA; $H(-CH=CH)_n-H$] is the prototypical compound. The insertion of ethynyl units into a PA scaffold leads to rodlike polymers, such as the polydiacetylenes [PDAs, $H(-C\equiv C-$

$CH=CH)_n-H$],[3,4] and the polytriacetylenes [PTAs, $H(-C\equiv C-CH=CH-C\equiv C)_n-H$][5-7] (see Scheme 1). It has been observed that these polyeneynes (PDAs, PTAs) show better thermal stability and solubility than the original polyenes (PAs), and, in addition, the capability to form functional derivatives with fully planar, sterically unhindered frameworks.[6]
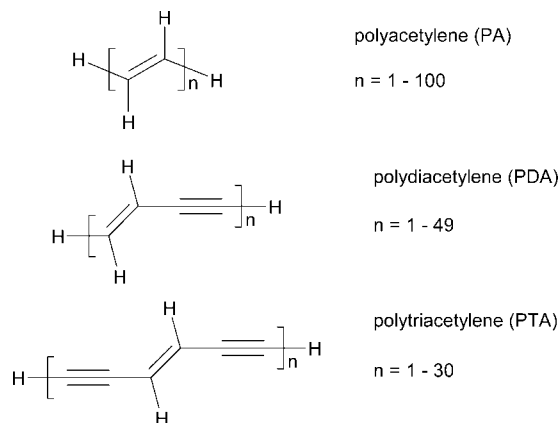
Obviously, the incorporation of ethynyl groups in the PA scaffold will affect the molecular as well as the electronic structure of these compounds. Properties such as the bond length alternation (BLA),[8] the maximum absorption wavelength (E_{max}),[9] and the second-order hyperpolarizabilities (γ)[10] were reported to differ substantially between polyenes and polyeneynes. It was also shown that γ and other

* Corresponding author.
† Università degli Studi di Milano-Bicocca.
‡ ETH Zürich.
§ University of Zürich.

Linearly π-Conjugated Systems

J. Chem. Theory Comput., Vol. 5, No. 3, 2009 **507**

Scheme 1. The Series of Oligomers Considered in This Study

polyacetylene (PA)

n = 1 - 100

polydiacetylene (PDA)

n = 1 - 49

polytriacetylene (PTA)

n = 1 - 30

properties saturate at shorter effective conjugation length (ECL) relative to PA, indicating that conjugation efficiency, i.e., the ability to promote electron delocalization along the backbone, is less pronounced.

These observations prompted us to explore the evolution of π-conjugation in PA, PDA, and PTA. For that matter, we studied the response of selected physical observables to the length of the backbone, and related these observations to the evolution of the delocalization energy along the π-conjugated chain using a new scheme based on the natural bond orbital (NBO) analysis.[11-13] The NBO analysis was shown to be a useful tool for the investigation of π-conjugation in earlier work.[8,14-16]

In this work we present and validate a new NBO-based scheme consisting of three different protocols for the evaluation of electron delocalization and conjugation efficiency in linearly π-conjugated chains. We will see that each π-conjugated backbone shows an orbital interaction energy profile which is characteristic for its type (PA, PDA, or PTA) as well as for its length. The orbital interaction profile may thus serve as a valuable molecular descriptor for this class of compounds. Furthermore, the scheme is general and transportable to other π-conjugated systems, including donor−acceptor functionalized ones.

2. Computational Details

In this work we study the oligomers of PA, PDA, and PTA with up to 180 carbon atoms. In the case of PDA, the hydrogen atom of the C≡C−H terminus is replaced by an ethynyl unit for better comparison with the other oligomers (note that with this definition the monomers of PDA and PTA are identical). Systems with 18, 30, 42, etc. carbon atoms are observed for all of the three types of backbones.

The geometry optimizations and the NBO analysis were performed within the DFT framework,[17] using the hybrid Becke three-parameters B3LYP functional[18-20] with a 6-31G(d,p) basis set of Gaussian orbitals.[21] The optical absorption properties were computed using Zerner's INDO/S method[22] on the B3LYP/6-31G(d,p) optimized geometries. In the ZINDO calculations, all occupied and virtual orbitals were retained in the active space. The excitation energies listed refer to the first allowed transition, which, in all cases considered, is a π−π* transition.

Polarizabilities (α) and second-order hyperpolarizabilities (γ) were computed on the B3LYP geometries using the coupled-perturbed (CP) Hartree−Fock approach[23] based on a semiempirical MNDO Hamiltonian.[24] The longitudinal polarizabilities and hyperpolarizabilities correspond to the tensor elements in the direction of the charge transfer axis (α_{zz} and γ_{zzzz} in our reference system) of the molecule. In order to compare computed and measured γ values, the theoretical values were multiplied by factors derived from the phenomenological approach.[25]

The DFT and ZINDO calculations were carried out using the Gaussian03 package,[26] while the calculations of polarizabilities and second-order hyperpolarizabilities were performed with the program MOPAC2000.[27] The NBO analysis was performed using the program NBO 5.0.[28]

The tendency of B3LYP to overestimate electron delocalization[29-32] as well as its failure to reproduce the polarizabilities and hyperpolarizabilities[33,34] of linearly conjugated systems are well-known. Various forms of long-range-corrected exchange functionals have been shown to overcome these problems.[35-37] At the same time, it is not obvious that there is *one single* DFT functional that makes excellent predictions for *all* observables considered here. In a recent study on PA chains, Tozer and co-workers demonstrate that the Coulomb-attenuated CAM-B3LYP DFT method[38] provides a much better estimate of the BLA,[35] but, on the other hand, also confirm the findings of Ma et al.[39] that the standard B3LYP HOMO−LUMO energies are much better suited to model the excitation energies for the long chains. This observation is of relevance here, as the NBO orbital interaction energies directly depend on the orbital energy differences.

Even though it is a small basis set, the 6-31G(d,p) basis has frequently been used in similar investigations, since the addition of more diffuse functions rather quickly leads to linear dependency issues.[35,36] It was recently shown[36] that the trend observed for the long-range-corrected B3LYP and the MP2 longitudinal polarizability and hyperpolarizability of PDA as a function of chain length is well preserved when switching from a 6-31G(d) to a 6-31+G(d) basis set.

Since this study is about reproducing trends in similar series of compounds rather than to present highest quality data on these observables for the oligomers of PA, PDA, and PTA, we resorted to semiempirical methods that appear to reproduce the available experimental data rather well (see also considerations on method performance in the respective sections of this article or ref 8). For short oligomers of PA, PDA, and PTA, for which experimental absorption spectra are available, the ZINDO calculations are in reasonable agreement with the experimental lowest allowed excitation energies. The polarizabilities and hyperpolarizabilities computed by means of an MNDO Hamiltonian reproduce the trend observed in the experiment rather well.[6,8]

Since PDA and PTA contain alternating single, double, as well as triple bonds, the traditional definition of the BLA needs to be extended. In earlier work on PTA oligomers,[8] we had introduced a generalized parameter δR defined as the difference between the averages of the saturated and the unsaturated bond lengths:

$$\delta R = [(C_D - C_T) + (C_T - C_T)]/2 - [(C\equiv C) + (C\equiv C)]/2 \tag{1}$$

where $(C_D - C_T)$ and $(C_T - C_T)$ represent the lengths of the single bonds in between a double and a triple bond or two triple bonds, respectively. For PDA, which only shows one kind of single bond, eq 1 is reduced to

$$\delta R = (C_D - C_T) - [(C=C) + (C\equiv C)]/2 \tag{2}$$

whereas for PA the standard definition applies

$$\delta R = (C-C) - (C=C) \tag{3}$$

The values of δR are always those in the *center* of the oligomers. On account of the different definitions given above, only the evolution of the δR for a given chain type will be observed; comparisons of δR for different types of backbones are to be made with care.

The properties of the oligomers considered in this work, at least to smaller chain length, have already been investigated extensively by other researchers[9,33,40–54] using different methodologies and levels of theory.

3. Details of the Analysis of Electron Delocalization and Conjugation Efficiency

The basic approach used for the analysis of electron delocalization in π-conjugated systems applied here is outlined in detail in earlier work.[15,55] In these articles we show that the π-delocalization energy can be evaluated either by means of the deletion of the weakly occupied π^* NBOs contained in the path, or by the summation of the interaction energies between the adjacent unsaturated orbitals along the pathway. The scheme presented also applies for σ-conjugation. In this work, however, we will exclusively focus on π-electron delocalization, since in the *through* conjugated systems considered here, in-plane σ-hyperconjugation is not expected to play a major role.

Whereas for the (quantitative) evaluation of π-electron delocalization various approaches have been proposed,[56–62] the conjugation efficiency, to the best of our knowledge, lacks a clear definition. It is generally understood as the ability of a backbone to promote electron delocalization. The ECL and the value of the property under consideration at infinite chain length offer a quantitative measure for the conjugation efficiency of a given backbone. A system with a backbone that promotes electron delocalization well, will, in general, show a large ECL as well as a significant evolution of the property considered.

The first estimate of conjugation efficiency therefore is in the response of the properties to chain length extension, i.e., the slope of the property as a function of chain length. For the systems studied here, those backbones whose properties show the strongest response to chain length extension will also show the largest ECL and the strongest evolution of the respective property.

In this research, we are using three different protocols to analyze π-conjugation presented in the next section.

π-Delocalization Energy Per Carbon Atom. The total π-delocalization energy (E_π) is evaluated by calculating the energies resulting from the deletion of *all* vertical π^* orbitals

Scheme 2. Schematic Representation of the PTA Polymer with the $\pi \rightarrow \pi^*$ Interactions Accounted for the Calculation of $E_\pi^{norm\,a}$
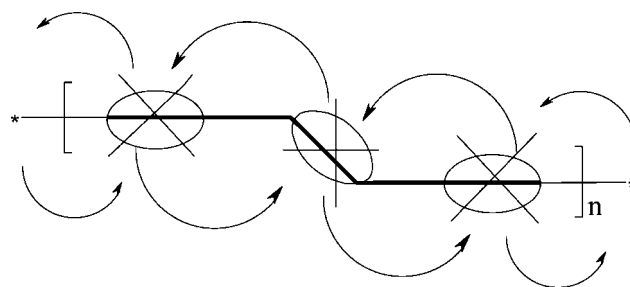
PTA; $E_\pi^{norm} = E_\pi / n(C)-2$

[a] In the scheme $n(C)$ stands for the number of carbon atoms in the oligomer. For PDA and PA, the interactions are accounted for in the same manner.

along the chain. To allow a direct comparison of the E_π values for the different oligomers, E_π is normalized to the number of $\pi \rightarrow \pi^*$ donor–acceptor orbital interactions in the chain, which corresponds to $n(C) - 2$, where $n(C)$ is the number of carbon atoms in the oligomer ($E_\pi^{norm} = E_\pi/n(C) - 2$; see Scheme 2).

The orbital interaction energy profiles make use of the donor–acceptor view of the chemical bond in NBO theory, which renders itself nicely to explore electron delocalization along a polymer chain. The (second order) orbital interaction energies (SOIE) between π and π^* donor/acceptor orbital pairs are given by the expression:

$$E_{SOIE_{ij}} = q_i \frac{F(i,j)^2}{\varepsilon_i - \varepsilon_j} \tag{4}$$

where i and j are the donor and the acceptor NBOs under consideration, respectively, ε_i and ε_j are the corresponding orbital energies, q_i is the donor orbital occupancy, and $F(i,j)$ is the element of the Fock matrix in the NBO basis connecting the interacting orbitals.

The interaction energies between neighboring unsaturated bonds along the backbone for 30-atom chains of the three oligomers considered here are shown in Figure 1. The evolution of the SOIE interactions along the chain defines a profile which is characteristic for the chain type and also for the chain length.

In PA, where the chain consists of identical unsaturated bonds, the orbital interactions will be very similar, varying slowly when moving from the terminal to the central part of the oligomer. If the chain is long enough, the orbital interaction energies in the core of the oligomer will reach an asymptotic value, which is the same for all oligomers of that type. On the other hand, in PDA or PTA the orbital interactions energies between double and triple bonds, and between triple and triple bonds, will differ considerably, leading to a more "rugged" profile of the chain. Again, all these specific interactions energies will vary slowly when moving toward the center of the oligomer, to finally reach their respective asymptotic values. Therefore, we will obtain interaction energy profiles that are characteristic for the type of chain as well as for its length. Note that in Figure 1 these
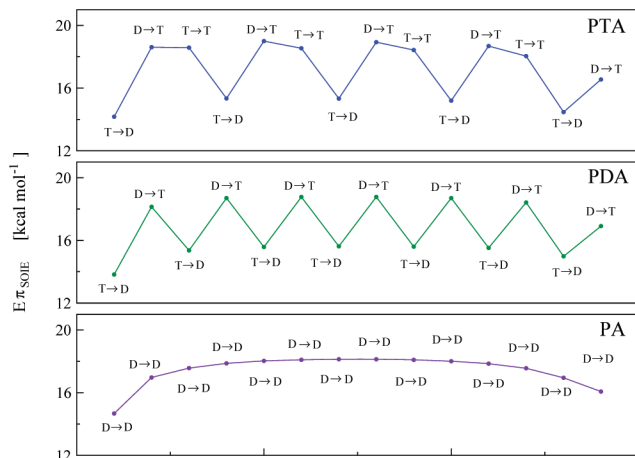
Linearly π-Conjugated Systems

J. Chem. Theory Comput., Vol. 5, No. 3, 2009 **509**

Figure 1. $\pi \rightarrow \pi^*$ SOIEs profile (in kcal mol^{-1}) along a fixed-length 30 carbon atoms backbone for PA (purple dots), PDA (green dots), and PTA (blue dots). The labels D → D, T → D, T → T, and D → T stand for the $\pi_{C=C} \rightarrow \pi^*_{C=C}$, $\pi_{C\equiv C} \rightarrow \pi^*_{C=C}$, $\pi_{C\equiv C} \rightarrow \pi^*_{C\equiv C}$, and $\pi_{C=C} \rightarrow \pi^*_{C\equiv C}$ interactions, respectively. The graph reports the $\pi \rightarrow \pi^*$ SOIEs determined by scanning the backbone from left to right. The profile corresponding to the scan in opposite direction is the mirror image to the one reported.

profiles are scanned from "left to right" along the chain, without considering the (symmetric) interactions in opposite direction.

Response of the Backbone to the Extension of the π-Conjugated Chain. To determine the response of the backbone to chain extension, the oligomers are partitioned into a core backbone and into two terminal π-conjugated units, as shown in Scheme 3. This allows the definition of a parameter $\Delta E\pi_{SOIE}$

$$\Delta E\pi_{SOIE} = \sum E\pi_{SOIE}^{core}(n+2) - \sum E\pi_{SOIE}(n) \quad (5)$$

where $\sum E\pi_{SOIE}^{core}(n + 2)$ is the sum of the $E\pi_{SOIE}$ energies between all vertical π orbitals of the core backbone in the oligomer $n + 2$, and $\sum E\pi_{SOIE}(n)$ is the sum of the $E\pi_{SOIE}$ energies between all vertical π orbitals of the oligomer of size n. The $E\pi_{SOIE}$ interactions to be included in the summations are shown in Scheme 3. For PTA and PDA an extra monomer unit covers six, respectively four more carbon atoms. For PA, the additional monomer unit was selected to cover six carbon atoms (as in PTA). The reference system is the geometry optimized oligomer of size n. This means that $\Delta E\pi_{SOIE}$ also takes into account the contribution of the geometry relaxation in response to the extension of the π-conjugation pathway. Clearly, the values of $\Delta E\pi_{SOIE}$ depend on the length of the terminal units assumed in the definition. However, we found that for different lengths of the terminal segments, the comparison of the values of $\Delta E\pi_{SOIE}$ and their evolution with respect to the number of carbon atoms is very similar, and therefore leads to the same observations (not shown). Also, the values of the SOIEs are functions of the $\varepsilon_i - \varepsilon_j$ energy gap (see eq 1), which, in turn, is dependent on the theoretical method adopted. However, from previous studies[15,55] we know that the B3LYP orbital interaction energies computed for the purpose of the comparison of similar compounds (polyenes and polyeneynes) appear to be adequate.

## 4. Evolution of the Molecular Properties as a Function of the Chain Length

Bond-Length Alternation. The evolution of δR, as defined in eqs 1−3, is reported as a function of the reciprocal number of carbon atoms ($1/C$) in Figure 2. δR of PA decreases to reach a constant value (zero gradient for δR vs $1/C$) at about 33 double bonds. For PDA and PTA the response of δR to chain length extension is nearly identical; δR converges to an effective conjugation length (ECL) of 20−22 double bonds for both compounds,[8] a value substantially smaller that the one of PA. The extrapolated infinite chain BLA for PDA and PTA is significantly larger than that of PA (0.106 and 0.078, respectively, versus 0.056 Å), but, due to the differences in the definition of the respective δR values, the comparison has to be made with care.

The BLA value extrapolated for a polymer of infinite chain length is in agreement with the finding of Tozer et al. using the same functional and basis set.[35] Using the CAM-B3LYP[38] and BHHLYP[18] functionals, these authors find an infinite chain value for the BLA of 0.087 and 0.089 Å, which is well within the experimental range of 0.08 ± 0.03 Å.[63] These results confirm the tendency of the generic B3LYP method to overestimate delocalization and presumably also the ECL. On the other hand, the present study does not confirm the presence of a minimum of the BLA before reaching the ECL (infinite chain value) as suggested by Tozer and co-workers.[35]

The evolution of the *first allowed excitation energy* (E_{max}) and the *HOMO−LUMO energy gap* as a function of the reciprocal number of carbon atoms of the oligomers investigated are reported in Figure 3. For short oligomers we observe excitation energies for PA that are close to those of PDA and PTA. As the oligomer chain increases, the excitation energy of PA decreases most rapidly, and, for the largest oligomers considered in this study, it is significantly lower than that calculated for the other two types of backbones. The excitation energy of PDA responds slightly faster than that of PTA to chain extension, but converges to the same value at a very large ECL (>75 unsaturated bonds). The extrapolated ZINDO/S value for the excitation energy of PA is equal to about 1.8 eV, in agreement with the experimental optical gap of 1.5−1.8 eV.[64,65]

The longitudinal polarizability α_L of a linearly π-conjugated compound is proportional to the length of the system for large oligomers.[33,44,66−68] This means that for these compounds the polarizability per unit length approaches an asymptotic value. Indeed, for all of the oligomers investigated in this work, the values of α_L divided by the number of carbon atoms of the backbone (α_L/C) appear to slowly converge to an asymptotic limit (Figure 4a). For short oligomers the values of α_L/C are very similar for all compounds. Upon increasing chain length, the value of α_L/C of PA evolves most rapidly, reaching an ECL of 38−40 double bonds, a value significantly higher than that extrapolated for PDA and PTA (28−30 unsaturated bonds). This is in good agreement with experiment[9] and other theoretical predictions.[45,52]

For short π-conjugated oligomers the longitudinal second-order hyperpolarizability γ_L follows the power law $\gamma_L = \gamma_m n^a$

Scheme 3. Schematic Representation of the Partitioning of a PTA Oligomer into a Core Backbone and Two Extra Terminal π-Conjugated Units[a]
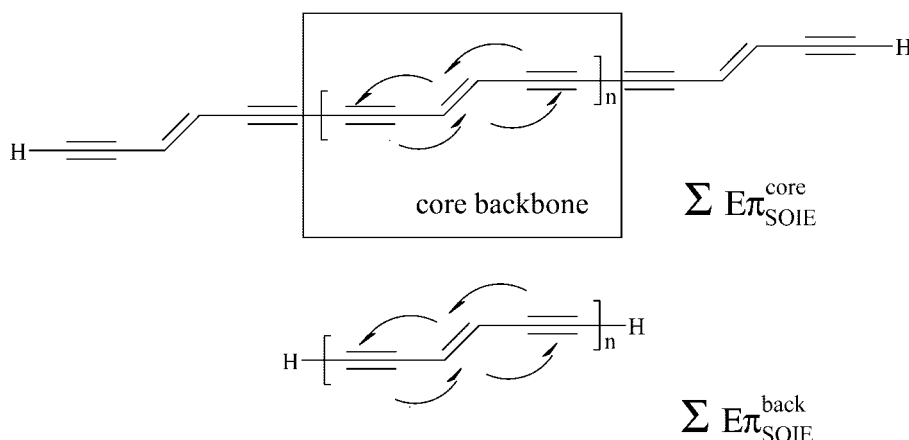
[a] $\Delta E\pi_{SOIE}$ is calculated as the difference between the $E\pi_{SOIE}$ of the core backbone ($\Sigma E\pi_{SOIE}^{core}$) and $E\pi_{SOIE}$ of an oligomer without the two terminal units ($\Sigma E\pi_{SOIE}^{back}$). For PDA and PA, $\Delta E\pi_{SOIE}$ is evaluated in the same manner.
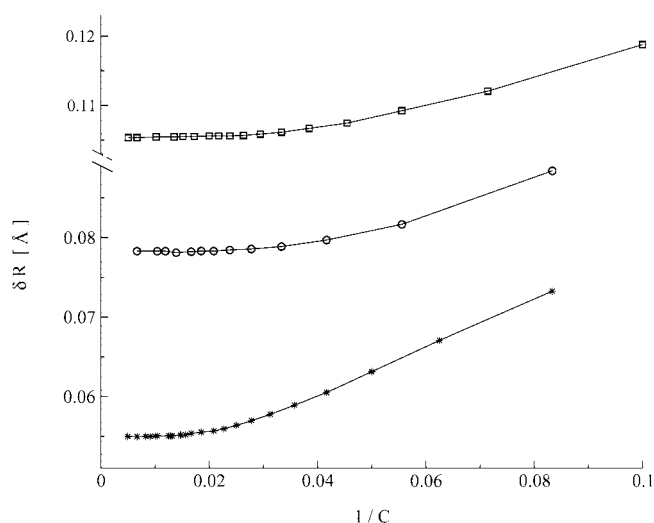

Figure 2. Evolution of the calculated δR parameter (in Å) as function of the reciprocal number of carbon atoms ($1/C$) for the PA (*), PDA (□),and PTA (○) oligomers at the B3LYP/6-31G(d,p) level of theory. The alternation parameter is determined for the central unit using eqs 1–3.

(where n is the number of oligomer units, and γ_m and a are constants).[69-71] For large oligomers, the γ_L values deviate from this power law, thus indicating inward saturation. In previous work[8] we showed that the γ values calculated for the PTA oligomers up to 54 carbon atoms are in satisfactory agreement with those determined from third harmonic generation (THG) and degenerate four-wave mixing (DFWM) measurements.[72] This observation is confirmed also for the longer chains considered here. Figure 4b reports the evolution of the values of γ_L per carbon atom of the backbone (γ_L/C) with respect to oligomer size. The trend is similar to that discussed above for α_L/C. The γ_L/C value of PA evolves much more rapidly than that of any other type of backbone. The γ_L/C values of the PDA and PTA oligomers again are very similar and converge to the same ECL. The extrapolation yields an ECL slightly larger than that evaluated for

the BLA, but more similar to the one discussed for the polarizability.

In summary, we see that for all of the properties investigated in this work (Table 1), the incorporation of an ethynyl group into a PA chain has a significant effect on the evolution of the backbone properties. This is reflected by the slope (gradient) of the various properties with respect to chain length extension as well as by the difference in ECL between PA and PDA/PTA. For PTA, we confirm the experimental observation of generally shorter ECLs relative to PA.[6,10] On the other hand, the insertion of a second triple bond when going from PDA to PTA, shows no additional impact on the values of the properties, at least as far as their evolution as a function of the chain length is concerned. For the excitation energies and the polarizabilities, we even observe convergence to the same value for the two backbones.

5. Analysis of π-Electron Delocalization in PA, PDA, and PTA Oligomers

For all compounds investigated, the π-delocalization energy per donor–acceptor interaction (E_π^{norm}; see Scheme 2 for definition of term) monotonically increases with increasing oligomer size (Figure 5). For short oligomers, PTA shows the largest E_π^{norm}, followed by PDA and PA. However, E_π^{norm} of PA evolves most rapidly with increasing oligomer size. Therefore, for longer chains PA surpasses PDA to nearly reach the infinite chain value of E_π^{norm} for PTA. This result supports the observation made on the basis of the computed molecular properties that the incorporation of triple bonds in the PA chain increases the π-delocalization energy, but that in larger chains of PDA and PTA π-electron delocalization is promoted less efficiently.

From the response of the backbone to the elongation of the chain length in terms of orbital interactions ($\Delta E\pi_{SOIE}$; eq 5), we see that for all oligomers investigated, $\Delta E\pi_{SOIE}$ converges to an asymptotic value (Figure 6). The addition of further units only has a constant effect (delocalization energy gained by connecting fragments to a saturated core) and does not lead to further enhancement of π-electron
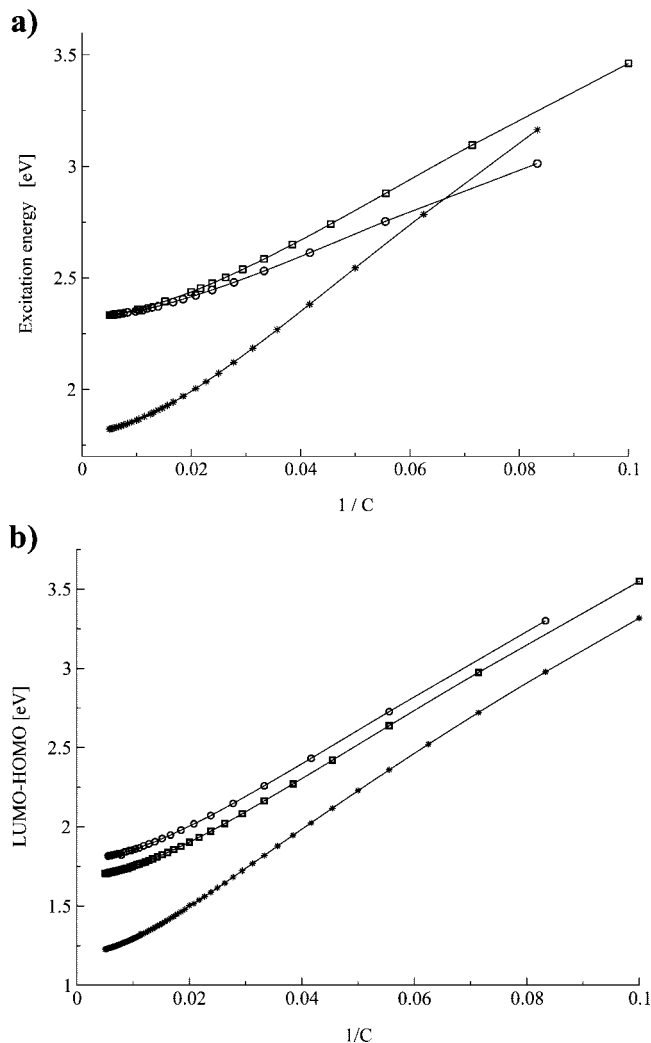
a)

b)

Figure 3. (a) Evolution of the calculated first allowed excitation energy (E_{max}) (in eV) as function of the reciprocal number of carbon atoms (1/C) for the PA (*), PDA (□), and PTA (○) oligomers computed at ZINDO level. (b) Evolution of the B3LYP LUMO-HOMO energy gap (in eV) as function of the reciprocal number of carbon atoms (1/C) for the PA (*), PDA (□), and PTA (○) oligomers.

delocalization in the backbone. Again, we see that $\Delta E\pi_{SOIE}$ of PA increases most rapidly to take a value significantly larger (about 8 kcal mol^{-1}) than that of the polyeneynes. The evolution of $\Delta E\pi_{SOIE}$ for PDA and PTA is similar, with PTA converging to a value of 2 kcal mol^{-1} lower than that of PDA. Given the much larger gradient of $\Delta E\pi_{SOIE}$ with respect to chain length, the PA backbone again appears to show the more enhanced π-conjugation efficiency, which is consistent with the observed evolution of the molecular properties.

Finally, the analysis of π-electron delocalization along the backbone in terms of $\pi \rightarrow \pi^*$ orbital interactions gives us more insight in how π-electron delocalization propagates along the different types of chains. The interaction energy profiles for the polyenes and the polyeneynes are vastly different. Whereas we have a "smooth" interaction energy profile for PA, we observe an oscillating ("rugged") profile for PDA and PTA. In the polyeneynes the $\pi_{C\equiv C} \rightarrow \pi^*_{C\equiv C}$ (T → T) and the $\pi_{C=C} \rightarrow \pi^*_{C\equiv C}$ (D → T) interaction energies
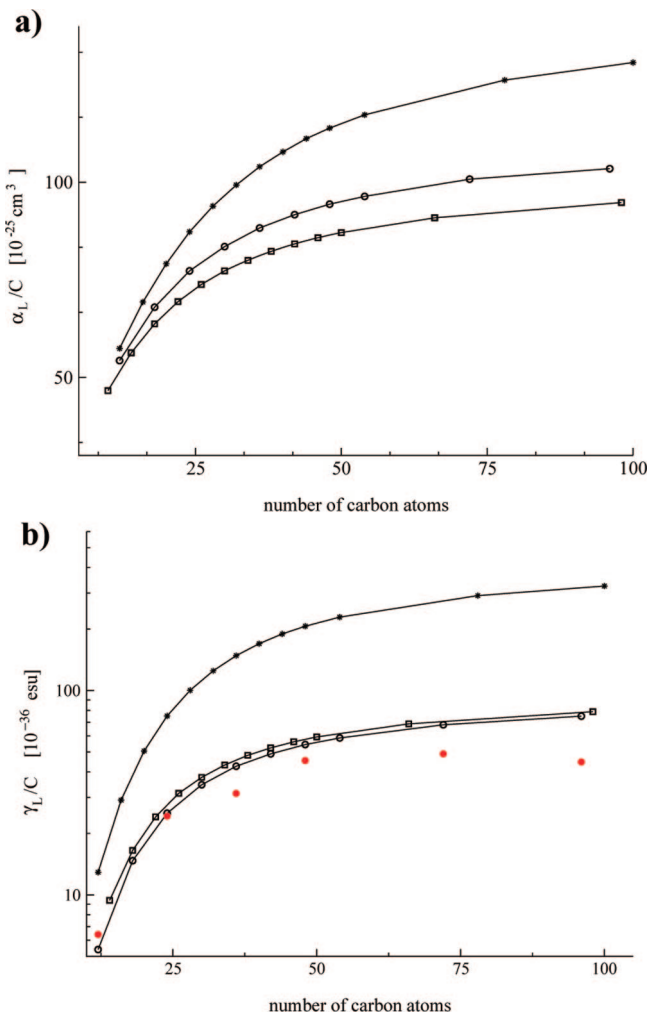
a)

b)

Figure 4. (a) Evolution of the calculated longitudinal polarizability per carbon atom of the backbone (α_L/C) (in 10^{-25} cm^3) as a function of the number of carbon atoms for PA (*), PDA (□), and PTA (○) oligomers computed at the CPHF-MNDO level of theory. (b) Evolution of the calculated longitudinal second-order hyperpolarizability per carbon atom of the backbone (γ_L/C) (in 10^{-34} esu) as a function of the number of carbon atoms for the PA (*), PDA (□), and PTA (○) oligomers computed at the CPHF-MNDO level of theory. The experimental values available for PTA are listed as single filled dots.

are considerably larger than the $\pi_{C'C} \rightarrow \pi^*_{C=C}$ (T → D) ones. This interaction is also weaker than the D → D one in PA. In the orbital interaction model used here, the comparatively weak T → D interactions in the polyeneynes will reduce delocalization relative to the polyene and therefore lower their conjugation efficiency.

For short oligomers, the sum of orbital interactions in the polyeneynes is still larger than in PA, leading to a larger value for the overall delocalization energy. For the extended oligomers, the reduced promotion of electron delocalization due to the relatively weak T → D interactions will reverse this situation in favor of PA (see also Figure 5). The observation that the D → D interaction energies in PA are lower than the T → T interaction energies in PTA is also in agreement with the conclusions reported in a recent study of von Schleyer et al.,[73] in which the π-delocalization energy

Table 1. Conjugation Efficiency in Terms of the Effective Conjugation Length (ECL), the Extrapolated Value for a Polymer of Infinite Chain Length, and the Gradient of the Properties with Respect to Chain Length Extension (Slope) for the Three Types of Backbones Investigated in This Work[a]

	PA			PDA			PTA		
	ECL[b]	$n = \infty$[c]	slope[d]	ECL[b]	$n = \infty$[c]	slope[d]	ECL[b]	$n = \infty$[c]	slope[d]
δR	~32	0.056	0.301 (32)	~21	0.106	0.199 (26)	~21	0.780	0.214 (24)
excitation energy	~49	1.81	18.6 (54)	~37	2.33	12.9 (50)	~34	2.33	9.5 (54)
LUMO−HOMO energy gap	~64	1.22	22.2	~50	1.70	19.0	~52	1.80	18.8
α/C	~57	135	—	~49	96	—	~51	107	—
γ/C	~82	348	—	~77	86	—	~77	82	—
$\Delta E\pi_{SOIE}$	~32	20.8	—	~21	12.7	—	~21	10.7	—
E_π^{norm}	—	15.8	−20.0	—	15.4	−11.9	—	15.9	−14.2

[a] δR in Å, excitation energies in eV, LUMO-HOMO gaps in eV, α/C in 10^{-25} esu, γ/C in 10^{-36} esu, $\Delta E\pi_{SOIE}$, and E_π^{norm} in kcal mol^{-1}. [b] The ECL indicates the number of unsaturated bonds for which the observable considered exceeds 99.9% of the infinite chain value. [c] Extrapolated value for a polymer of infinite chain length based on 4th-order polynomials (correlation coefficient greater than 0.999). [d] Slope of the linear segment of the curves (in $1/C$ representation) with the maximum number of carbon atoms considered for the linear regression.
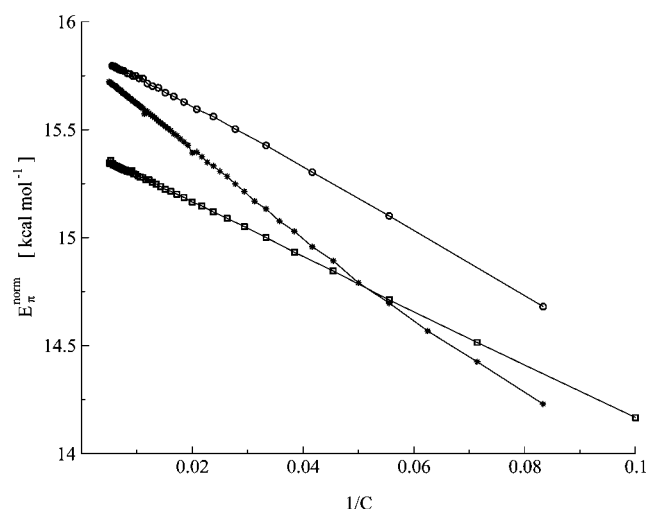
Figure 5. E_π^{norm} values as a function of reciprocal number of carbon atoms for the PA (*), PDA (□), and PTA (○) oligomers, computed at the B3LYP/6-31G(d,p) level of theory (see also Scheme 2).
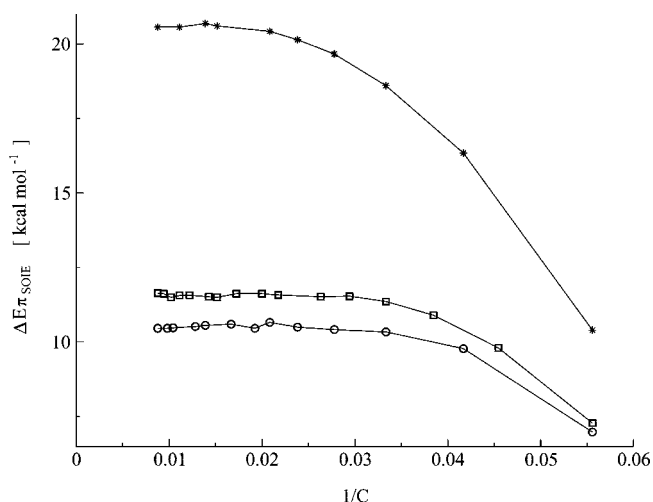
Figure 6. Evolution of $\Delta E\pi_{SOIE}$ (eq 5) as a function of the reciprocal number of carbon atoms for the PA (*), PDA (□), and PTA (○) oligomers computed at the B3LYP/6-31G(d,p) level of theory. The definition of backbones and terminal groups is given in Scheme 3.

of 1,3-butadiyne and 1,3-butadiene were compared by means of the computed heats of hydrogenation.
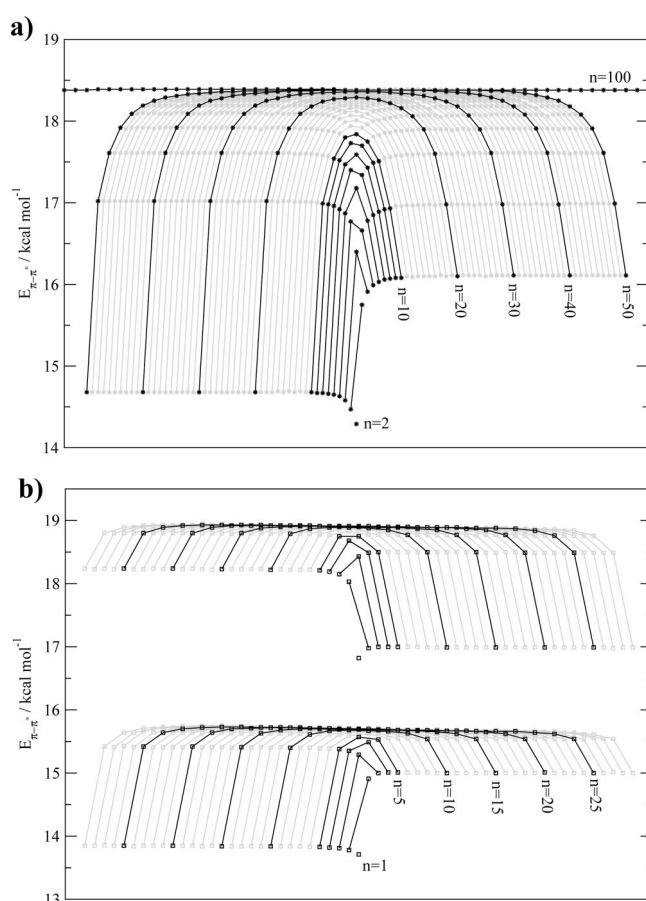
Figure 7. $\pi \rightarrow \pi^*$ interaction energies (in kcal mol^{-1}) for all oligomers of PA (up to $n = 50$) and PDA (up to $n = 29$). As in Figure 1, the backbone is scanned from left to right, only showing the symmetry-unique interaction energies. The graph a starts with butadiene ($n = 2$; listed in the center), which shows just one unique orbital−orbital interaction, and ends with the interaction energies of the pentadecamer ($n = 50$) of PA. In addition, the interaction energies in the core of the hectamer ($n = 100$) are shown. In panel b, the double−triple bond (upper part) and triple−double bond interactions (lower part) are shown from the monomer up to the $n = 29$ system.

From Figure 7a,b, which shows *all* orbital interaction energies for *all* oligomers of PA and PDA, we see that for both compounds each specific interaction converges to a specific asymptotic value. For PA, the interaction energy between the

Linearly π-Conjugated Systems

J. Chem. Theory Comput., Vol. 5, No. 3, 2009 **513**

outermost double bond (donor) and its next neighbor (acceptor), for example, converges to a value of 14.6 kcal mol^{-1} for chains larger than 20 atoms, whereas the interaction between orbitals in the center (core) of the chain converges to a value 3.8 kcal mol^{-1} higher for chains longer than 30 atoms. Obviously, the asymptotic value of the interaction energies increases as one moves toward the core of the backbone. (see also Figure 1 for the 30 carbon atom chain); at the same time we observe that the interaction energies converge more slowly.

For PDA and PTA (not shown), we observe a very similar convergence pattern for the orbital interactions. Relative to PA, the asymptotic values for the interactions in the core of the PDA backbone are somewhat higher for the D → T bond interactions (19.0 kcal mol^{-1}), but distinctly lower (15.8 kcal mol^{-1}) for the T → D bond interactions. Also, the margin between the interaction energies among the inner (core) and the outer bonds is much smaller in PDA (and also in PTA). This observation is yet another expression of the reduced response of PDA and PTA to chain length extension.

Finally, the stability of the converged values of the interaction energies is an illustration of the reliability as well as the numerical stability of the models used here.

In summary, from the three schemes of analysis we see that the incorporation of an ethynyl group into a PA chain increases the total delocalization energy, but, at the same time, introduces relatively weak T → D interactions in the backbone, which are responsible for the reduced conjugation efficiency in PDA. The insertion of a second triple bond (PDA → PTA) does not add any more "damage", and therefore the properties of PDA and PTA show similar conjugation efficiency.

6. Conclusions

The schemes of analysis introduced here show that the insertion of ethynyl groups into a PA chain increases the total π-delocalization energy for short PDA and PTA oligomers, but, very importantly, reduces the efficiency with which π-electron delocalization is promoted. The less efficient π-electron delocalization is also responsible for the generally shorter ECL observed for the properties of the polyeneynes relative to the polyenes. Accordingly, all physical observables computed for PA evolve more rapidly as a function of the oligomer size, and converge to an ECL larger than those computed for PDA and PTA. The insertion of a second ethynyl group into the PDA chain does not further modulate the efficiency with which π-electron delocalization is promoted. The loss of conjugation efficiency observed for the polyeneynes is the result of the relatively weak orbital interactions involving the triple bond π orbitals as donors and the double bond π* orbitals as acceptors (T → D interaction; see Figures 1 and 6). These weak orbital interactions represent the *bottleneck* in the delocalization of charge along the chain. The orbital interaction energy profile appears to be a very promising scheme of analysis, also because it is characteristic for the compound investigated. It may thus render the basis for a molecular descriptor for this class of compounds.

References

(1) *Handbook of Conducting Polymers*, 3th ed.; Skotheim, T. A., Reynolds, J., Eds.; CRC Press: Boca Raton, FL, 2007.

(2) Blythe, T.; Bloor, D. *Electrical Properties of Polymers*; Cambridge University Press: Cambridge, UK, 2005.

(3) *Polydiacetylene*; Cantow, H. J., Ed.; Springer-Verlag: Berlin, 1984.

(4) Bässler, H. *Polydiacetylenes*; Blood, D., Chance, R. R., Eds.; Nijhoff: Dordrecht, 1985, p 135.

(5) Schreiber, M.; Anthony, J.; Diederich, F.; Spahr, M. E.; Nesper, R.; Hubrich, M.; Bommeli, F.; Degiorgi, L.; Wachter, P.; Kaatz, P.; Bosshard, C.; Günter, P.; Colussi, M.; Suter, U. W.; Boudon, C.; Gisselbrecht, J.-P.; Gross, M. *Adv. Mater.* **1994**, *6*, 786.

(6) Martin, R. E.; Gubler, U.; Cornil, J.; Balakina, M. Y.; Boudon, C.; Bosshard, C.; Gisselbrecht, J.-P.; Diederich, F.; Günter, P.; Gross, M.; Brédas, J.-L. *Chem. Eur. J.* **2000**, *6*, 3622.

(7) Nielsen, M. B.; Diederich, F. *Chem. Rev.* **2005**, *105*, 1837.

(8) Bruschi, M.; Giuffreda, M. G.; Lüthi, H. P. *ChemPhysChem* **2005**, *6*, 511.

(9) Fujii, A.; Hydarat, R.; Sonoda, T.; Fujisawa, T.; Ozaki, M.; Vardeny, Z. V.; Teraguchi, M.; Masuda, T.; Yoshino, K. *Synt. Met.* **2001**, *116*, 95.

(10) Samuel, I. D. W.; Ledoux, I.; Dhenaut, C.; Zyss, J.; Fox, H. H.; Schrock, R. R.; Silbey, R. J. *Science* **1994**, *265*, 1070.

(11) Reed, A. E.; Weinhold, F. *J. Chem. Phys.* **1983**, *78*, 4066.

(12) Reed, A. E.; Curtiss, L. A.; Weinhold, F. *Chem. Rev.* **1988**, *88*, 899.

(13) Weinhold, F.; Landis, C. R. *Valency and Bonding: A Natural Bond Orbital Donor-Acceptor Perspective*; Cambridge University Press: Cambridge, UK, 2005.

(14) Limacher, P. A.; Lüthi, H. P. *J. Phys. Chem. A* **2008**, *112*, 2913.

(15) Bruschi, M.; Giuffreda, M. G.; Lüthi, H. P. *Chem. Eur. J.* **2002**, *8*, 4216.

(16) Bruschi, M.; Giuffreda, M. G.; Lüthi, H. P. *Chimia* **2005**, *59*, 539.

(17) Parr, R. G.; Yang, W. *Density Functional Theory of Atoms and Molecules*; Oxford University Press: New York, 1989.

(18) Becke, A. D. *J. Chem. Phys.* **1993**, *98*, 5648.

(19) Lee, C.; Yang, W.; Parr, R. G. *Phys. Rev. B* **1988**, *37*, 785.

(20) Becke, A. D. *Phys. Rev. A* **1988**, *38*, 3098.

(21) Hehre, W. J.; Ditchfield, R.; Pople, J. A. *J. Chem. Phys.* **1972**, *56*, 2257.

(22) Zerner, M. C. *Semiempirical Molecular Orbital Methods; Reviews of Computational Chemistry*; VCH: New York, 1991; *Vol. 2*; p 313.

(23) Kurtz, H. A.; Steward, J. J. P.; Dieter, K. M. *J. Comput. Chem.* **1990**, *11*, 82.

(24) Dewar, M. J. S.; Thiel, W. *J. Am. Chem. Soc.* **1977**, *99*, 4899.

(25) Willetts, A.; Rice, E., J.; Burland, E. J.; Shelton, M., D. *J. Chem. Phys.* **1992**, *97*, 7590.

(26) Frisch, M. J.; Trucks, G. W.; Schlegel, H. B.; Scuseria, G. E.; Robb, M. A.; Cheeseman, J. R. ; Montgomery J.A. Jr.; Vreven, T.; Kudin, K. N.; Burant, J.C.; Millam, J. M.; Iyengar, S. S.; Tomasi, J.; Barone, V.; Mennucci, B.; Cossi, M.; Scalmani, G.; Rega, N.; Petersson, G. A.; Nakatsuji, H.; Hada, M.; Ehara, M.; Toyota, K.; Fukuda, R.; Hasegawa, J.; Ishida, M.; Nakajima, T.; Honda, Y.; Kitao, O.; Nakai, H.; Klene, M.; Li, X.; Knox, J. E.; Hratchian, H. P.; Cross, J. B.; Bakken, V.; Adamo, C.; Jaramillo, J.; Gomperts, R.; Stratmann, R. E.; Yazyev, O.; Austin, A. J.; Cammi, R.; Pomelli, C.; Ochterski, J. W.; Ayala, P. Y.; Morokuma, K.; Voth, G. A.; Salvador, P.; Dannenberg, J. J.; Zakrzewski, V. G.; Dapprich, S.; Daniels, A. D.; Strain, M. C.; Farkas, O.; Malick, D. K.; Rabuck, A. D.; Raghava- chari, K.; Foresman, J. B.; Ortiz, J. V.; Cui, Q.; Baboul, A. G.; Clifford, S.; Cioslowski, J.; Stefanov, B. B.; Liu, G.; Liashenko, A.; Piskorz, P.; Komaromi, I.; Martin, R. L.; Fox, D. J.; Keith, T.; Al.Laham, M. A.; Peng, C. Y.; Nanayakkara, A.; Challacombe, M.; Gill, P. M. W.; Johnson, B.; Chen, W.; Wong, M. W.; Gonzalez, C.; Pople, J. A. *Gaussian 03, Revision C.02*; Gaussian, Inc.: Wallingford CT, 2004.

(27) Stewart, J. J. *MOPAC 2000*; Fujitsu Ltd: Tokyo, 1999.

(28) Glendening, E. D. Badenhoop, J., K. Reed, A. E. Carpenter, J. E. Bohmann, J. A. Morales, M. Weinhold, F. *NBO 5.0*; Theoretical Chemistry Institute, University of Wisconsin: Madison, WI, 2001.

(29) Geskin, M., V.; Dkhissi, A.; Brédas, J. L. *Int. J. Quantum Chem.* **2003**, *91*, 351.

(30) Geskin, V. M.; Grozema, F. C.; Siebbeles, S. D. A.; Beljonne, D.; Brédas, J. L.; Cornil, J. *J. Phys Chem. B* **2005**, *109*, 20237.

(31) Lundberg, M.; Siegbahn, P. E. M. *J. Chem. Phys.* **2005**, *122*, 224103.

(32) Mori-Sánchez, P.; Cohen, A. J.; Yang, W. *Phys. Chem. Lett.* **2008**, *100*, 146401.

(33) Champagne, B.; Perpète, E. A.; van Gisbergen, S. J. A.; Baerends, J. E.; Snijders, J. G.; Soubra-Ghaoui, C.; Robins, K.; Kirtman, B. *J. Chem. Phys.* **1998**, *109*, 10489.

(34) Champagne, B.; Perpète, A. E.; Jacquemin, D.; van Gisbergen, S. J. A.; Baerends, J. E.; Soubra-Ghaoui, C. *J. Phys Chem. A* **2000**, *104*, 4755.

(35) Peach, M. J. G.; Tellgren, E. I.; Salek, P.; Helgaker, T.; Tozer, D. J. *J. Phys. Chem. A* **2007**, *111*, 11930.

(36) Kirtman, B.; Bonness, S.; Ramirez-Solis, A.; Champagne, B.; Matsumoto, H.; Sekino, H. *J. Chem. Phys.* **2008**, *128*, 114108.

(37) Jacquemin, D.; Perpète, E. A.; Scalmani, G.; Frisch, M. J.; Kobayashi, R.; Adamo, C. *J. Chem. Phys.* **2007**, *126*, 144105.

(38) Yanai, T.; Tew, D. P.; Handy, N. C. *Chem. Phys. Lett.* **2004**, *393*, 51.

(39) Ma, J.; Li, S.; Jiang, Y. *Macromolecules* **2002**, *35*, 1109.

(40) Barford, W. *Electronic and Optical Properties of Conju- gated Polymers; International Series of Monographs on Physics*; Clarendon Press: Gloucestershire, UK, 2005.

(41) *Conjugated Polymers: The Novel Science and Technology of Highly Conducting and Nonlinear Optically Active Materials*; Brédas, J.-L., Silbey, R., Eds.; Kluwer Academic Publishers: Dordrecht, 1991.

(42) Suhai, S. *Phys. Rev. B* **1995**, *51*, 16553.

(43) Choi, C. H.; Kertesz, M.; Karpfen, A. *J. Chem. Phys.* **1997**, *107*, 6712.

(44) Champagne, B.; Perpète, E. A. *Int. J. Quantum Chem.* **1999**, *75*, 441.

(45) Lu, D. Q.; Marten, B.; Ringnalda, M.; Friesner, R. A.; Goddard, W. A. *Chem. Phys. Lett.* **1996**, *257*, 224.

(46) Su, W. P.; Schrieffer, J. R.; Heeger, A. J. *Phys. Rev. Lett.* **1979**, *42*, 1698.

(47) Su, W. P.; Schrieffer, J. R.; Heeger, A. J. *Phys. Rev. B* **1980**, *22*, 2099.

(48) Mintmire, J. W.; White, C. T. *Phys. Rev. B* **1987**, *35*, 4180.

(49) Perpète, E. A.; Champagne, B. *J. Mol. Struct. (Theochem)* **1999**, *487*, 39.

(50) Shirakawa, H.; Louis, E. J.; MacDiarmid, A. G.; Chiang, C. K.; Heeger, A. J. *J. Chem. Soc., Chem. Commun.* **1977**, *16*, 578.

(51) Shirakawa, H. *Angew. Chem., Int. Ed.* **2001**, *40*, 2575.

(52) Ma, J.; Li, S.; Jiang, Y. *Macromolecules* **2002**, *35*, 1109.

(53) Tretiak, S.; Mukamel, S. *Chem. Rev.* **2002**, *102*, 3171.

(54) Bredas, J.-L.; Beljonne, D.; Coropceanu, V.; Cornil, J. *Chem. Rev.* **2004**, *104*, 4971.

(55) Giuffreda, M. G.; Bruschi, M.; Lüthi, H. P. *Chem. Eur. J.* **2004**, *10*, 5671.

(56) Mo, Y.; Peyerimhoff, S. D. *J. Chem. Phys.* **1998**, *109*, 1687.

(57) Gobbi, A.; Frenking, G. *J. Am. Chem. Soc.* **1994**, *116*, 9275.

(58) Mo, Y.; Jiao, H.; Lin, Z.; Schleyer, P. v. R. *Chem. Phys. Lett.* **1998**, *289*, 383.

(59) Fernández, I.; Frenking, G. *Chem. Eur. J.* **2006**, *12*, 3617.

(60) Schleyer, P. v. R.; Maerker, C.; Dransfeld, A.; Jiao, H.; van Eikema Hommes, N. J. R. *J. Am. Chem. Soc.* **1996**, *118*, 6317.

(61) Fernández, I.; Frenking, G. *J. Org. Chem.* **2006**, *71*, 2251.

(62) Heine, T.; Schleyer, P. v. R.; Corminboeuf, C.; Seifert, G.; Reviakine, R.; Weber, J. *J. Phys Chem. A* **2003**, *107*, 6450.

(63) Yannoni, C. S.; Clarke, T. C. *Phys. Rev. Lett.* **1983**, *51*, 1191.

(64) Hori, Y.; Noda, K.; Kobayashi, S.; Taniguchi, H. *Tetrahedron Lett.* **1969**, 3563.

(65) Fincher, C. R.; Chen, C. E.; Heeger, A. J.; MacDiarmid, A. G.; Hastings, J. B. *Phys. Rev. Lett.* **1982**, *48*, 100.

(66) Perpète, E. A.; Champagne, B. *J. Chem. Phys.* **1997**, *107*, 2463.

(67) Champagne, B.; Mosley, D.; Vračko, M.; Andrè, J.-M. *Phys. Rev. A* **1995**, *52*, 178.

(68) Kudin, N., K.; Car, R.; Resta, R. *J. Chem. Phys.* **2005**, *122*, 134907.

(69) Kanis, D. R.; Ratner, M. A.; Marks, T. J. *Chem. Rev.* **1994**, *94*, 195.

(70) Morley, J. O. *Int. J. Quantum Chem.* **1993**, *46*, 19.

(71) Brédas, J.-L.; Adant, C.; Tackx, P.; Persoons, A.; Pierce, B. M. *Chem. Rev.* **1994**, *94*, 243.

(72) Gubler, U.; Bosshard, C.; Günter, P.; Balakina, M. Y.; Cornil, J.; Brédas, J.-L.; Martin, R. E.; Diederich, F. *Opt. Lett.* **1999**, *24*, 1599.

(73) Jarowski, P. D.; Wodrich, M. D.; Wannere, C. S.; Schleyer, P. v. R.; Houk, K. N. *J. Am. Chem. Soc.* **2004**, *126*, 15036.